



UNIVERSITÀ POLITECNICA DELLE MARCHE
Repository ISTITUZIONALE

Interlayer bonding characterization of interfaces reinforced with geocomposites in field applications

This is the peer reviewed version of the following article:

Original

Interlayer bonding characterization of interfaces reinforced with geocomposites in field applications / Canestrari, F.; Cardone, F.; Gaudenzi, E.; Chiola, D.; Gasbarro, N.; Ferrotti, G.. - In: GEOTEXTILES AND GEOMEMBRANES. - ISSN 0266-1144. - STAMPA. - 50:1(2022), pp. 154-162. [10.1016/j.geotexmem.2021.09.010]

Availability:

This version is available at: 11566/295083 since: 2024-04-29T13:18:44Z

Publisher:

Published

DOI:10.1016/j.geotexmem.2021.09.010

Terms of use:

The terms and conditions for the reuse of this version of the manuscript are specified in the publishing policy. The use of copyrighted works requires the consent of the rights' holder (author or publisher). Works made available under a Creative Commons license or a Publisher's custom-made license can be used according to the terms and conditions contained therein. See editor's website for further information and terms and conditions.

This item was downloaded from IRIS Università Politecnica delle Marche (<https://iris.univpm.it>). When citing, please refer to the published version.

(Article begins on next page)

1 *Interlayer bonding characterization of interfaces reinforced with*
2 *geocomposites in field applications*

3
4 *F. Canestrari¹, F. Cardone¹, E. Gaudenzi*¹, D. Chiola², N. Gasbarro³, G. Ferrotti¹*

5 ¹ Department of Civil and Building Engineering and Architecture, Università Politecnica delle
6 Marche, 60131 Ancona, Italy; f.canestrari@staff.univpm.it; f.cardone@staff.univpm.it;
7 g.ferrotti@staff.univpm.it;

8 ² Autostrade Tech, Via A. Bergamini 50, 00159 Roma, Italy, davide.chiola@autostrade.it;

9 ³ Autostrade per l'Italia, Via A. Bergamini 50, 00159 Roma, Italy,

10 nicoletta.gasbarro@autostrade.it;

11 *Corresponding author.

12 E-mail address: e.gaudenzi@pm.univpm.it (E. Gaudenzi¹)

13 ¹ Department of Civil and Building Engineering and Architecture, Università Politecnica delle
14 Marche, 60131 Ancona, Italy;

15
16 Abstract

17 Geocomposites are extensively used in asphalt pavements as they provide significant long-
18 term pavement benefits. Indeed, when correctly installed, geocomposites enhance road
19 pavement performance thanks to their waterproofing properties, stress absorbing membrane
20 interlayer (SAMI) action and improved mechanical strength of the pavement. Nevertheless, the
21 presence of an interlayer causes de-bonding effects that negatively influence the overall
22 pavement characteristics. This paper presents an experimental investigation aimed at

23 comparing the interlayer bonding characteristics of four different geocomposites with an
24 unreinforced reference configuration, laid on an Italian motorway section, in which the
25 reinforcement depth and the lower layer surface condition (milled or new) were also varied.
26 Interlayer shear strength (ISS) was measured, on both cores and laboratory produced
27 specimens, through Leutner and Ancona Shear Testing Research and Analysis (ASTRA)
28 equipment. The ISS results showed that geocomposites can be successfully applied directly on
29 milled surfaces. Moreover, the application of a normal stress, as in the ASTRA device, tends to
30 mitigate any difference related to the specimen heterogeneity. Finally, existing laws, which
31 correlate the results obtained with different shear equipment on unreinforced interfaces, were
32 generalized by considering the presence of geocomposites and the corresponding ISS
33 specification limits were proposed for both ASTRA and Leutner test.

34

35 KEYWORDS: Asphalt pavements, Interlayer bonding, Geocomposites, Reinforcements,
36 Interface Shear Strength, Field Performance

37

38 *1. Introduction*

39 Reinforcement systems are often employed within asphalt pavement layers for
40 maintenance and rehabilitation purpose, with the aim of preventing or delaying the
41 development of cracks. Nowadays, increasing traffic loadings generate accelerated functional
42 and structural distresses, requiring frequent and expensive maintenance activities. In this
43 scenario, geocomposites can be used as cost-effective, long-lasting and sustainable
44 rehabilitation methods. Indeed, they should allow an extension on the service life or a
45 reduction in the overall pavement thickness (Correia & Zornberg, 2016), also providing
46 significant environmental benefits.

47 Geocomposites are usually obtained as a combination of geomembranes with
48 geosynthetics (e.g. geogrids), in order to achieve benefits in terms of stress absorbing and

49 waterproofing effects (due to presence of the geomembrane) as well as improved tensile
50 properties provided by the geosynthetic reinforcement (Canestrari et al., 2016; Khodaii et al.,
51 2009; Pasquini et al., 2014). Nevertheless, the presence of any type of reinforcement at the
52 interface causes an interlayer de-bonding effect (Brown et al. 2001; Canestrari et al., 2012;
53 Ferrotti et al., 2011; Khodaii et al., 2009; Noory et al., 2017) that influences pavement
54 response in terms of stress-strain distribution, resulting in near-surface cracking (Ingrassia et
55 al., 2020; Park et al, 2021; Pasquini et al., 2015).

56 A good interlayer bonding condition is a key factor when the asphalt pavement
57 performance is considered as good bonding allows a better distribution of the bending stresses
58 induced by the traffic loads. In fact, improved interlayer bonding conditions can guarantee a
59 decrease in the tensile strain at the bottom of each layer (Uzan et al., 1978) and reduce the
60 slippage effect which can occur at the interface, especially in areas where high shear forces
61 can arise due to braking and turning of heavy vehicle. In synthesis, when de-bonding occurs at
62 the interface, the asphalt pavements can no longer act as a monolithic system and provide the
63 expected load-bearing capacity, leading to a more rapid pavement failure (Ferrotti et al., 2011;
64 Ran et al., 2019; Zamora-Barraza et al., 2010). For this reason, the evaluation of interlayer
65 bonding is fundamental for a proper estimation of the pavement service life, especially when
66 interlayer reinforced systems are employed (Noory et al. 2019).

67 The evaluation of interlayer bonding can be carried out through many different equipment
68 characterized by different parameters, such as test speeds, specimen size and loading
69 conditions (Canestrari et al., 2013; "Optim. Tack Coat HMA Place.," 2012; Raab et al., 2009).

70 The most common and simple device has been designed by Leutner in 1979 (R. Leutner, 1979)
71 and allows performing pure direct shear test without the application of normal stresses at the
72 interface. However, several studies showed that a normal stress approximately equal to 0.2
73 MPa can be recommended when performing interlayer bonding characterization, to better
74 reproduce the most critical traffic loading conditions (Ozer et al., 2012, Karshenas et al., 2014).

75 For this reason, the Ancona Shear Testing Research and Analysis (ASTRA) device ([Canestrari et](#)
76 [al., 2005](#); [Santagata et al., 1993](#)), able to carry out direct shear tests with the application of
77 different levels of normal load, is more appropriate to better simulate the real in situ
78 conditions.

79 Within a RILEM (Réunion Internationale des Laboratoires d'Essais et de Recherches sur les
80 Matériaux et les Constructions) interlaboratory test on interlayer bonding ([Canestrari et al.,](#)
81 [2013](#)), analytical laws were proposed to model the effect of several parameters (such as
82 normal load, specimen size, temperature and test speed) on the Interlayer Shear Strength (ISS)
83 measured with different shear testing equipment. These laws were obtained for interfaces
84 located between two new asphalt concrete layers laid on field trials ("new on new"), with and
85 without tack coat application and in absence of interlayer systems such as geocomposites.

86 Given this background, this research study aims at evaluating the bonding characteristics of
87 asphalt pavements when rehabilitation techniques with geocomposites are considered. For
88 this purpose, a field trial with the application of four different geocomposites was built on an
89 Italian motorway section, by considering different surface conditions for the lower layer
90 (milled or new) and different positions of the reinforcement within the rehabilitated pavement
91 structure, since as these variables have a crucial incidence in absorbing tensile strains
92 mobilized during loading ([Saride & Kumar, 2017](#)). Cores taken from the field trial and
93 laboratory prepared specimens (with the same materials used in the field) were subjected to
94 shear tests with both Leutner and ASTRA devices, by comparing the interlayer performance of
95 geocomposites with an unreinforced reference configuration. Then, the existing correlations
96 between different shear testing equipment ([Canestrari et al., 2013](#)) were generalized by
97 considering the presence of geocomposites. Finally, ISS specification limits were proposed for
98 both Leutner and ASTRA device when geocomposites interlayer systems are considered.

99
100

101 *2. Field trial*

102 The experimental investigation is based on the construction of a field trial along an in-
103 service Italian motorway consisting of three sections with initial homogeneous characteristics,
104 identified by using project historical data and visual inspections.

105 The sections, named as T1, T4 and T6, are located on the first right lane (width equal to 4
106 m), as represented in Figure 1. Maintenance works planned on Sections T1 and T6 represent a
107 typical maintenance activity which can be completed in one night (avoiding too much
108 discomfort to users), after the milling of the existing pavement layers (Figure 2). The two
109 Sections (T1 and T6) have the same stratigraphy (11 cm base course and 4 cm porous wearing
110 course) but a different subgrade bearing capacity. Specifically, a Heavy Weight Deflectometer
111 (HWD) campaign, carried out immediately after the milling operations, provided a subgrade
112 elastic modulus equal to 2670 MPa and 3720 MPa for Section T1 and T6, respectively.

113 Differently, section T4 represents a typical full-depth repair maintenance work consisting of
114 the milling of the existing pavement followed by the construction of two base layers of 10 cm
115 and 15 cm, respectively, and one porous wearing course of 4 cm. Since it is laid in three layers,
116 it is not compatible with the one-night construction.

117 Each section was further divided into five subsections, characterized by different interface
118 configurations (Figure 2). Four different types of geocomposites available on the market for
119 road applications (coded as A, B, C and D) were compared with a reference unreinforced
120 configuration (coded as N), where an unmodified bituminous emulsion was spread at the
121 interface. In each section, the position of the geocomposites inside the pavement structure
122 was also varied, as shown in Figure 2. Specifically, the geocomposites were applied on a milled
123 lower layer surface in sections T1 and T6 (below the new base layer) and on a new surface in
124 section T4 (between the two new base layers). It is worth noting that geocomposites were
125 directly positioned over the lower layer surface without the application of a tack coat which
126 seems to provide no improvement in the overall interlayer performance of the system, as

127 shown by [Pasquini et al., 2014](#); [Pasquini et al., 2015](#). This procedure also guarantees
128 compliance with the deadlines for carrying out the rehabilitation works, thanks to the reduced
129 number of activities to be performed in one night.

130 *3. Materials*

131 *3.1 Asphalt concrete*

132 The asphalt concrete (AC) used as base course is characterised by a maximum aggregate
133 size equal to 31.5 mm, with a 30% of Reclaimed Asphalt (RA).

134 The RA was an un-fractioned 0/14 class deriving from the milling of old binder and base
135 motorway layers. The bitumen contained in the RA was an SBS polymer modified bitumen and
136 its content was equal to 5% by aggregate weight.

137 The total bitumen content of the AC is equal to 4.05% by the aggregate weight, and the
138 maximum theoretical density was 2.501 g/cm³.

139 The porous asphalt concrete used as wearing course is characterized by a maximum
140 aggregate size of 20 mm. The total bitumen content is equal to 5.25% by the aggregate weight
141 and a 0.3% by aggregate weight of cellulose-glass fibre was added to prevent drain-down
142 problems. In both cases, an SBS polymer modified bitumen was employed as virgin binder,
143 whose characteristics are listed in Table 1.

144

145 *3.2 Unmodified bituminous emulsion*

146 The cationic bituminous emulsion used as tack coat in the reference unreinforced interface
147 configuration N, is classified as C55B3 according to EN 13808 and is composed of 55% of
148 unmodified residual bitumen. It is characterized by a medium-fast breaking class (class 3) and
149 was applied with a dosage of 0.6 kg/m² (0.33 kg/m² of residual bitumen), typical value for new
150 construction applications. The characteristics of the emulsion and of the residual bitumen are
151 shown in Table 2.

152

153 *3.3 Geocomposites*

154 The geocomposites used in this study are coded as A, B, C and D and are supplied by
155 producers in rolls 10÷15 m long and 1 m wide. They are classified as self-thermo-adhesive
156 membranes and are provided with a removable silicone bottom film that preserves the
157 thermo-adhesive compound (Figure 3.a). The upper surfaces of geocomposites B, C and D
158 (Figure 3.b) are coated with sand and minerals which avoid sticking the roll coils and act as
159 intermediary adhesion. Differently, the geocomposite A has a non-stick selvedge as upper
160 surface (Figure 3.b). The reinforcement of geocomposites A, C and D consists of a fiberglass
161 mesh, whereas the geocomposite B is characterised by a continuous sheet of non-directional
162 glass fibers and high-duty non-woven polyester fabric. In addition, the products A, B and D are
163 isotropic, whereas the geocomposite C is slightly more resistant to tensile stress in the
164 transversal direction. The main characteristics of the geocomposites are summarized in
165 Table 3.

166

167 *4. Specimen preparation*

168 *4.1 Field cores*

169 After the laying of the field trial, six cores with a nominal diameter of 100 mm were
170 extracted for each interface configuration (N, A, B, C and D) from each section (T1, T4 and T6)
171 for a total of 90 cores, characterized by different types of interface (unreinforced/reinforced
172 and milled/new surface).

173 However, the cores sampled from section T1 were strongly disturbed during the extraction
174 of the specimens from the core drill (by grabbing and pulling down the lower layer), making
175 even impossible the use of some of them for laboratory investigations, due to the complete
176 separation of the layers. Therefore, it is very important to pay attention during the coring
177 activities to preserve the specimen interface from separation and avoid gathering incorrect
178 testing results.

179 Before testing, each core was resized by cutting the upper layer about 40 mm above the
180 geosynthetic position and the lower layer about 40 mm below the geosynthetic position, to
181 obtain specimens with a total height equal to about 80 mm. Both layers are characterized by
182 an air void content ranging between 5 and 6%.

183 *4.2 Laboratory specimens*

184 The materials used for the construction of the field trial were also employed in laboratory
185 to obtain cylindrical specimens in order to carry out a laboratory investigation on the same
186 unreinforced and reinforced interface configurations (N, A, B, C and D).

187 Double-layered square slabs (305x305 mm²) were prepared through a Roller Compactor
188 according to the EN 12697-33 standard. The underlying layer was compacted with a thickness
189 of 40 mm and a target air void content of 5%. It was then cooled at room temperature for 3
190 hours before applying the tack coat (configuration N) or the geocomposites (A, B, C and D) on
191 its surface. A 40 mm upper layer was then compacted with the same target air void content
192 (5%). The compaction direction was then marked to carry out shear tests by applying interface
193 shear displacements along the direction parallel to the traffic flow in the field. A set of five
194 double-layered slabs were compacted, one for each interface configuration, i.e. one slab for
195 the unreinforced reference interface (N) and one slab for each type of geocomposite (A, B, C
196 and D). From each slab, five cylindrical specimens with a nominal diameter of 100 mm were
197 cored. This condition was coded as T4_lab as the lower layer surface is new and can be
198 compared with the cores extracted from section T4, where the geocomposites were applied on
199 the surface of the new lower base course.

200

201 *5. Experimental program and test methods*

202 The interlayer bonding characteristics of geocomposite-reinforced interfaces (A, B, C and D)
203 were compared with a reference unreinforced configuration (N) for evaluating the
204 effectiveness of asphalt pavement rehabilitation techniques carried out with geocomposites.

205 This comparison was performed on both laboratory-produced specimens and cores extracted
206 from the field trial described in Section 2. Moreover, a comparison between lower layer
207 surface conditions (milled or new) was also carried out for all the five interface configurations
208 (reference N with tack coat, geocomposite A, geocomposite B, geocomposite C and
209 geocomposite D).

210 Two different types of shear tests were used to measure the Interlayer Shear Strength (ISS):
211 the Leutner device and the Ancona Shear Testing Research and Analysis (ASTRA) device. The
212 same number of specimens were tested with both equipment in each configuration and
213 surface condition, as shown in Table 4. As above-mentioned, the cores extracted from section
214 T1 were disturbed by the drilling operation, reducing the number of available specimens.

215 The Leutner is a direct “pure” shear device (Figure 4a), compliant with the European
216 Standard [prEN 12697-48](#). The lower part moves upward with a constant displacement rate
217 equal to 50.8 ± 2 mm/min, while the upper part is in contrast with a load cell, which produces
218 the shear load at the interface without normal stress. The shear force and the shear
219 displacement are continuously measured during the test, allowing the determination of the
220 ISS, i.e. the maximum interlayer shear stress calculated as ratio between the maximum shear
221 force and the specimen interface area. The shear device can test cylindrical specimen with 150
222 mm or 100 mm nominal diameter. The tests were performed at a temperature of 20 °C and all
223 the specimens were conditioned in a climatic chamber for at least 4 hours before testing.

224 The ASTRA device (Figure 4b) is a direct shear box, compliant with the European Standard
225 [prEN 12697-48](#). The double-layered specimen is located between two half-boxes, opportunely
226 spaced to create an unconfined interlayer shear zone. During the test, the lower half-box is
227 moved with a constant horizontal displacement rate equal to 2.5 mm/min, while a constant
228 vertical load can be applied in order to obtain the target confining normal stress. Cylindrical
229 specimens with a nominal diameter of 100 mm can be tested. The horizontal force, the
230 horizontal displacement and the vertical displacement are recorded during the test, allowing

231 the determination of the ISS. The whole apparatus is located in a climatic chamber for the
232 temperature control. The tests were performed in standard conditions, corresponding to the
233 application of a normal stress equal to 0.2 MPa and a temperature of 20 °C ([UNI/TS 11214](#)). All
234 the specimens were conditioned at 20 °C in a climatic chamber for at least 4 hours before
235 testing.

236

237 *6 Results and Analysis*

238 *6.1 Leutner test results*

239 The average values of ISS and the corresponding error bars obtained with the Leutner
240 device for all the lower layer surface conditions (T1, T4, T6 and T4_lab) and interface
241 configurations (N, A, B, C and D) are shown in Figure 5.

242 As above-mentioned, the results of section T1 cannot be considered reliable because the
243 interface of the cores was highly disturbed during their extraction from the core drill, as
244 demonstrated by ISS values lower than those of T6 (identical to T1), especially for the
245 reinforced specimens. For this reason, T1 results are reported in white in Figure 5 and are only
246 shown for comparison with T6, in order to highlight the relevance of the coring activities.

247 As expected, the unreinforced interface configuration N is characterized by the highest ISS
248 value in all the conditions tested as compared to the reinforced interface configuration, due to
249 the de-bonding effect provided by the geocomposites ([Brown et al., 2001](#); [Canestrari et al.,
250 2012](#); [Ferrotti et al., 2011](#); [Khodaii et al., 2009](#)). Moreover, the interface N showed higher
251 strengths in the new lower layer surface condition (T4) with respect to the milled one (T6). This
252 is probably due to the “fresh” modified bitumen of the AC laid as new lower layer, which is
253 more influential than the roughness induced by the milling operations. On the contrary,
254 section T6 showed higher ISS values than section T4 in the presence of geocomposites (except
255 for D configuration), supporting the possibility of applying the geocomposites directly on the

256 top of milled surfaces, unlike other widely used reinforcement types (e.g. geogrid) which
257 require a levelling thin layer before their application (Pasquini et al., 2015).

258 The geocomposite C applied on section T6 showed the lowest de-bonding effect, providing
259 ISS values similar to the unreinforced interface N. On the contrary, the other reinforced
260 interfaces (A, B and D) provided a higher de-bonding compared to the unreinforced interface
261 N, as testified by lower ISS values. Differently, the laboratory prepared specimens (T4_lab)
262 showed similar ISS values for the geocomposites B, C and D, whereas the geocomposite A
263 provided the lowest value.

264

265 *6.2 ASTRA test results*

266 The average ISS results of ASTRA tests and the corresponding error bars for all the
267 conditions tested are presented in Figure 6.

268 Also in this case, the ASTRA results of section T1 (in white in Figure 6) cannot be considered
269 because the cores were highly disturbed during their extraction from the core drill.

270 As for the Leutner test, the unreinforced interface N is characterized by the highest ISS
271 values in all the conditions studied, even though it also showed the highest dispersion values.
272 This can lead to the conclusion that the application of geocomposites (having lower
273 dispersions) could mitigate differences related to specimen production or core extraction.

274 Geocomposites A, C and D applied over the milled surface (T6) provided similar ISS values,
275 which are slightly higher than those obtained for the geocomposite B, whose composition
276 could probably cause lower adhesion properties with the milled surface. In fact, the
277 geocomposite B is the only one that does not have a reinforcement grid but is composed of a
278 continuous and quite rigid sheet of non-directional glass fibres and high-duty non-woven
279 polyester fabric. For this reason, it probably establishes lower adhesion with the milled
280 surface, creating a higher separation effect, which is expressed in lower ISS values. When a
281 more regular surface is considered, as in the case of section T4, analogous ISS values were

282 obtained for all the reinforced interfaces, with slightly higher strengths for the geocomposite
283 B. However, the substantially equivalent results obtained for the two field lower layer surface
284 conditions (milled T6 and new T4) in the reinforced interface configurations (A, B, C and D),
285 demonstrated that the presence of the geocomposites tends to mitigate also differences
286 between milled and new lower layer surface, leading to the conclusion that they can be
287 successfully applied directly on the top of milled surfaces. Differently, the unreinforced
288 interface N showed slightly higher strengths for the section T4 (new), probably due to the
289 availability of “fresh” modified bitumen on the lower layer surface.

290 The ISS results obtained on specimens prepared in laboratory (T4_lab) showed that
291 geocomposites B and D provided the higher strengths between the reinforced interfaces,
292 whereas A and C provided almost identical performance.

293

294 *7 Influence of testing speed and normal stress on ISS*

295 As above-mentioned, in standard conditions, Leutner and ASTRA tests are carried out with
296 different testing speed (50.8 and 2.5 mm/min, respectively) and normal stress σ_n applied
297 (0.0 MPa and 0.2 MPa, respectively). The higher dispersion of Leutner results (Figure 5) with
298 respect to ASTRA results (Figure 6) allows observing that the application of the normal stress
299 $\sigma_n = 0.2$ MPa in the ASTRA tests seems to mitigate possible differences linked to the
300 heterogeneity of the specimens.

301 In this section, existing laws which correlate ISS values obtained with different shear testing
302 equipment in the case of unreinforced interfaces and new lower layer surface ([Canestrari et](#)
303 [al., 2013](#)), are generalized by considering also the presence of geocomposites at the interface.

304 The interlaboratory test on interlayer bonding carried out within the RILEM Technical
305 Committee "Advances in Interlaboratory Testing and Evaluation of Bituminous Materials"
306 ([Canestrari et al., 2013](#)), provided Eq. (1) which allows obtaining the ISS value at a generic

307 testing speed v_x (ISS_{vx}) by knowing the ISS at the speed v_1 (ISS_{v1}), in absence of normal
 308 stress:

$$309 \quad ISS_{vx} = ISS_{v1} \cdot \left(\frac{v_x}{v_1}\right)^{0.22} \quad (1)$$

310 By applying Eq. (1) to the Leutner results measured in laboratory at 50.8 mm/min
 311 ($ISS_{Leut50.8}$), the ISS associated with a Leutner test performed at 2.5 mm/min ($ISS_{Leut2.5}$) can
 312 be obtained through Eq. (2):

$$313 \quad ISS_{Leut2.5} = ISS_{Leut50.8} \cdot \left(\frac{2.5}{50.8}\right)^{0.22} \quad (2)$$

314 [Canestrari et al., 2013](#) also found further relationship, which considers the influence of the
 315 normal stress. Specifically, the ISS value when a normal stress σ_n is applied (in this case,
 316 ISS_{ASTRA}) can be obtained by knowing the ISS value found in absence of normal stress at the
 317 same testing speed (in this case, $ISS_{Leut2.5}$), as follows:

$$318 \quad ISS_{ASTRA} = (1 + 0.38 \cdot \sigma_n) \cdot ISS_{Leut2.5} + (0.74 \cdot \sigma_n) \quad (3)$$

319 where the parameter $(1+0.38 \cdot \sigma_n)$ is associated with the contribution of the cohesion
 320 (which includes also the dilatancy, equal to $0.38 \cdot \sigma_n$) and the parameter $(0.74 \cdot \sigma_n)$ with the
 321 residual friction ([Canestrari et al., 2005](#)). The laws defined by [Canestrari et al., 2013](#) for
 322 unreinforced interfaces were also confirmed by [Ortiz-Ripolla et al., 2020](#) even after the
 323 conclusion of the RILEM project.

324 The generalization of Eq. (2) and Eq. (3) for interfaces with geocomposites can be
 325 performed by introducing three parameters α_1 , α_2 and α_3 , as shown in Eq. (4) and Eq. (5):

$$326 \quad ISS_{Leut2.5} = ISS_{Leut50.8} \cdot \left(\frac{2.5}{50.8}\right)^{\alpha_1} \quad (4)$$

$$327 \quad ISS_{ASTRA} = (1 + \alpha_2 \cdot \sigma_n) \cdot ISS_{Leut2.5} + (\alpha_3 \cdot \sigma_n) \quad (5)$$

328 where $\sigma_n = 0.2$ MPa and α_1 , α_2 , α_3 were obtained by means of least squares optimization
 329 between the ASTRA testing results $(ISS_{ASTRA})_{meas}$ obtained with T4 and T4_lab specimens
 330 and the corresponding ASTRA values $(ISS_{ASTRA})_{calc}$ calculated with Eq. (5), as a function of
 331 the $ISS_{Leut2.5}$ values obtained by introducing in Eq. (4) the Leutner test results related to the

332 same testing conditions (T4 and T4_lab). The measured data and the results of the data
 333 analysis are summarized in Table 5, which allowed the determination of the following values
 334 for the three parameters: $\alpha_1 = 0.35$; $\alpha_2 = 0.20$; $\alpha_3 = 0.73$, calculated for $\sigma_n = 0.2$ MPa.

335

336 It can be observed that the values obtained for α_1 , α_2 and α_3 are consistent and
 337 meaningful when compared with the corresponding parameters obtained in previous study for
 338 unreinforced interfaces. In fact, a higher value of α_1 (0.35 versus 0.22 of the unreinforced
 339 interface) can be explained by the presence of the geocomposite, which is rich in bitumen and
 340 tends to amplify the effects of loading speed thanks to its viscoelasticity. The presence of a
 341 higher bitumen amount in the geocomposites also tends to reduce the asphalt mixture
 342 interlocking, causing a reduction of the dilatancy contribution, as shown by the reduction of
 343 the value α_2 (0.20 versus 0.38). Finally, in the case of geocomposites, characterized by non-null
 344 values of residual cohesion (Pasquini et al., 2014; Pasquini et al., 2015), the α_3 value is not
 345 directly associated with the residual friction but with the overall interlayer shear strength after
 346 the interface failure (combination of residual cohesion and residual friction).

347 By plotting the testing results $(ISS_{ASTRA})_{meas}$ and the calculated $(ISS_{ASTRA})_{calc}$ ASTRA
 348 values, it emerges that the data points are very close to the equality line, highlighting the good
 349 agreement between the measured and calculated data. Therefore, the practical equations to
 350 be used to correlate ISS results obtained with different shear equipment in the case of
 351 interfaces reinforced with geocomposites can be written, when $\sigma_n = 0.2$ MPa, as follows:

$$352 \quad \tau_{Leut2.5} = \tau_{Leut50.8} \cdot \left(\frac{2.5}{50.8}\right)^{0.35} \quad (6)$$

$$353 \quad \tau_{ASTRA} = (1 + 0.20 \cdot \sigma_n) \cdot \tau_{Leut2.5} + (0.73 \cdot \sigma_n) \quad (7)$$

354

355 *8 Technical Specification limits for ISS values*

356 Although proper interlayer bonding conditions are fundamental to guarantee good asphalt
 357 pavement performance, only a limited number of European Countries have adopted minimum

358 specification limits. All of them are based on the results obtained with the Leutner device or
359 with similar equipment, such as the Swiss Layer-Parallel Direct Shear (LPDS) apparatus.
360 Specifically, Germany and Switzerland technical specifications ([07 ZTV Asphalt-StB, 2007](#))
361 require that the ISS value obtained with Leutner test performed on field cores with a diameter
362 of 150 mm must be ≥ 0.85 MPa for the upper interface (i.e. between wearing and binder
363 course) and ≥ 0.65 MPa for lower interfaces (e.g. between binder and base course).
364 Differently, in the United Kingdom (UK), the technical specifications ([MCDHW, 2018](#)) require
365 ISS ≥ 1.0 MPa for interfaces located at depths ≤ 75 mm, and ISS ≥ 0.50 MPa for interfaces
366 located at greater depths.

367 Since geocomposites are characterized by a high dosage of bituminous materials to ensure
368 stress absorbing and waterproofing effects, their application is not recommended in
369 correspondence of the upper interface where a high bonding level is required. For this reason,
370 the UK criterion which considers ISS ≥ 0.50 MPa for interfaces located at depths greater than
371 75 mm was selected in this study as specification limit for Leutner tests. The corresponding
372 minimum specification limit to consider when performing ASTRA tests in standard conditions
373 ($\sigma_n = 0.2$ MPa) is equal to 0.33 MPa, which is obtained by applying Eq. (6) and Eq. (7) starting
374 from $\tau_{Leut50.8} = 0.50$ MPa.

375 In order to check if these limits can be considered suitable for verifying the field
376 requirements of interfaces reinforced with geocomposites, ASTRA and Leutner test results of
377 section T4 (new lower layer surface) were plotted in Figure 8. The analysis of the plot shows
378 that the minimum value of 0.50 MPa (taken from the literature) for Leutner device and
379 0.33 MPa (derived from Eqs. (6) and (7)) for ASTRA equipment, can be likely used as
380 “equivalent” specification limits in the evaluation of the field performance after
381 geocomposites application. Moreover, the experimental data of section T6 (Figure 8) shows
382 that the generalization proposed for interfaces with geocomposites on new lower layer surface
383 seems to be applicable in the case of milled lower layer surface as well.

384 Nevertheless, it is also necessary to investigate if during the laboratory qualification phase,
385 aimed at selecting the most appropriate geocomposite to be used in the field, these limits
386 need to be revised.

387 The comparison between the laboratory produced specimens and the corresponding field
388 cores was thus performed in parity of new lower layer surface condition, by plotting the results
389 obtained for T4_lab and T4 condition, respectively. Figure 9 shows that the field cores (T4)
390 without reinforcement (configuration N) are characterized by higher strengths than the
391 analogous laboratory specimens (T4_lab). On the contrary, the field cores of the reinforced
392 interface configurations (A, B C and D) are characterized by lower ISS values with respect to
393 the specimens prepared in laboratory, for both ASTRA and Leutner test. This is due to the
394 possibility of applying more properly the geocomposites in laboratory with respect to the field
395 condition, guaranteeing higher strengths.

396 Therefore, during the laboratory qualification phase, more restrictive criteria for the
397 definition of specification limits must be defined in order to achieve the required field
398 performance. The results shown in Figure 9.a can be used for the definition of these pre-
399 qualification limits for the Leutner test. Specifically, an increase by 50% of the value accepted
400 for field cores, i.e. 0.75 MPa, was reasonably proposed as specification limit for the
401 qualification phase of laboratory produced specimens, based on the comparison of the data
402 collected from the Leutner test for Sections T4_lab and T4 (Figure 5). Analogously, Eqs. (6) and
403 (7) can be used to obtain the qualification phase specification limit for ASTRA test, by
404 considering $\tau_{Leut50.8} = 0.75$ MPa. A value equal to 0.42 MPa was obtained and reported in
405 Figure 9.b.

406 The defined ISS minimum specification limits for interfaces reinforced with geocomposites
407 are summarized in Table 6. The analysis of Figure 9 shows that all laboratory specimens and
408 cores meet the proposed ISS minimum specification limits and, given this promising outcome,
409 their validation by further laboratory and/or field investigation is recommended.

410

411

412

413 *9 Conclusions*

414 This research aimed at evaluating the effectiveness of asphalt pavement rehabilitation
415 techniques by using different geocomposites. The interlayer bonding characteristics of four
416 different geocomposites were compared with an unreinforced reference configuration, by
417 using laboratory compacted specimens and cores taken from a field trial built on an Italian
418 motorway section consisting of three distinct sections, each characterised by a different
419 reinforcement position and lower layer surface conditions (new or milled). The interlayer shear
420 strength (ISS) was measured through Leutner and Ancona Shear Testing Research and Analysis
421 (ASTRA) equipment, allowing the following conclusions to be drawn:

- 422 – the application of geocomposites causes a de-bonding effect at the interface of asphalt
423 concrete pavements proved by the reduction of ISS values;
- 424 – geocomposites can be successfully applied directly on the top of milled surfaces as they can
425 mitigate differences related to specimen characteristics and lower layer surface conditions.
426 Moreover, this operation allows the speeding up of maintenance activities while avoiding
427 users discomfort and satisfying construction needs;
- 428 – the application of a normal stress during shear tests, as in the case of ASTRA device, can
429 reduce the dispersion of the ISS results;
- 430 – the laws which correlate the results obtained with different shear testing equipment in the
431 case of unreinforced interfaces were generalized for Leutner and ASTRA test results by
432 considering the presence of geocomposites;
- 433 – ISS minimum technical specification limits for interfaces reinforced with geocomposites
434 were proposed for Leutner and ASTRA tests, both in the qualification phase and in the

435 performance field assessment (after pavement rehabilitation). These limits are intended as
436 initial proposal that has to be validated with further investigations.

437

438

439 Acknowledgements

440 The activities presented in this paper were sponsored by Autostrade per l'Italia S.p.A. (Italy),
441 which gave both financial and technical support within the framework of the Highway
442 Pavement Evolutive Research (HiPER) project. The results and opinions presented are those of
443 the authors.

444

445 *References*

446 07 ZTV Asphalt-StB. (2007). *Zusätzliche Technische Vertragsbedingungen und Richtlinien für*
447 *den Bau von Verkehrsflächenbefestigungen aus Asphalt. Forschungsgesellschaft für*
448 *Straßen- und Verkehrswesen Arbeitsgruppe Asphaltbauweisen.*

449 Brown, S.F., Thom, N.H., Sanders, P. J. (2001). A study of grid reinforced asphalt to combat
450 reflection cracking. *J. Assoc. Asphalt Paving Technol.*, 70, 543–569.

451 Canestrari, F., Ferrotti, G., Abuaddous, M., & Pasquini, E. (2016). Geocomposite-reinforcement
452 of polymer-modified asphalt systems. *8th RILEM Bookseries*, 11.

453 https://doi.org/10.1007/978-94-017-7342-3_31

454 Canestrari, F., Ferrotti, G., Lu, X., Millien, A., Partl, M. N., Petit, C., Phelipot-Mardelé, A., Piber,
455 H., & Raab, C. (2013). Mechanical testing of interlayer bonding in asphalt pavements. In
456 *Advances in Interlaboratory Testing and Evaluation of Bituminous Materials. State-of-the-*
457 *Art Report of the RILEM Technical Committee 206-ATB.* [https://doi.org/10.1007/978-94-](https://doi.org/10.1007/978-94-007-5104-0_6)
458 [007-5104-0_6](https://doi.org/10.1007/978-94-007-5104-0_6)

459 Canestrari, F., Ferrotti, G., Partl, M. N., & Santagata, E. (2005). Advanced testing and
460 characterization of interlayer shear resistance. *Transportation Research Record; 1929(1)*,
461 69–78. <https://doi.org/10.3141/1929-09>

462 Canestrari, F., Pasquini, E., & Belogi, L. (2012). Optimization of geocomposites for double-
463 layered bituminous systems. *7th RILEM Bookseries, 2*, 1229. [https://doi.org/10.1007/978-](https://doi.org/10.1007/978-94-007-4566-7_117)
464 [94-007-4566-7_117](https://doi.org/10.1007/978-94-007-4566-7_117)

465 Correia, N. S., & Zornberg, J. G. (2016). Mechanical response of flexible pavements enhanced
466 with Geogrid-reinforced asphalt overlays. *Geosynthetics International, 23(3)*, 183–193.
467 <https://doi.org/10.1680/jgein.15.00041>

468 Ferrotti, G., Canestrari, F., Virgili, A., & Grilli, A. (2011). A strategic laboratory approach for the
469 performance investigation of geogrids in flexible pavements. *Construction and Building*
470 *Materials, 25(5)*, 2343–2348. <https://doi.org/10.1016/j.conbuildmat.2010.11.032>

471 Ingrassia, L. P., Virgili, A., & Canestrari, F. (2020). Effect of geocomposite reinforcement on the
472 performance of thin asphalt pavements: Accelerated pavement testing and laboratory
473 analysis. *Case Studies in Construction Materials, 12*(February), e00342.
474 <https://doi.org/10.1016/j.cscm.2020.e00342>

475 Karshenas, A., Carolina, N., Cho, S., Carolina, N., Tayebali, A. A., Carolina, N., Guddati, M. N.,
476 Carolina, N., & Kim, Y. R. (2014). The importance of normal confinement on shear bond
477 failure of interface in multilayer asphalt pavements. *Transport. Res. Rec.: J. Transport. Res.*
478 *Board, 2456(1)*, 170–177.

479 Khodaii, A., Fallah, S., & Moghadas, F. (2009). Geotextiles and Geomembranes Effects of
480 geosynthetics on reduction of reflection cracking in asphalt overlays. *Geotextiles and*
481 *Geomembranes, 27(1)*, 1–8. <https://doi.org/10.1016/j.geotexmem.2008.05.007>

482 MCDHW. (2018). *Manual of Contract Documents for highway works volume 2 notes for*

483 *guidance on the specification for highway Works.*

484 Noory, A., Moghadas Nejad, F., & Khodaii, A. (2017a). Evaluation of shear bonding and
485 reflective crack propagation in a geocomposite reinforced overlay. *Geosynthetics*
486 *International*, 24(4), 343–361. <https://doi.org/10.1680/jgein.17.00007>

487 Noory, A., Moghadas Nejad, F., & Khodaii, A. (2019). Evaluation of geocomposite-reinforced
488 bituminous pavements with Amirkabir University Shear Field Test. *Road Materials and*
489 *Pavement Design*, 20(2), 259–279. <https://doi.org/10.1080/14680629.2017.1380690>

490 Optimization of Tack Coat for HMA Placement. (2012). In *Optimization of Tack Coat for HMA*
491 *Placement*. <https://doi.org/10.17226/13652>

492 Ortiz-Ripolla, J., Miró, R., & Martínez, A. H. (2020). Semi-empirical method for the calculation
493 of shear stress, stiffness and maximum shear strength of bituminous interfaces under in-
494 service conditions. *Construction and Building Materials*, 258.
495 <https://doi.org/10.1016/j.conbuildmat.2020.120374>

496 Ozer, H., Al-Qadi, I. L., Wang, H., & Leng, Z. (2012). Characterisation of interface bonding
497 between hot-mix asphalt overlay and concrete pavements: Modelling and in-situ
498 response to accelerated loading. *International Journal of Pavement Engineering*, 13(2),
499 181–196. <https://doi.org/10.1080/10298436.2011.596935>

500 Park B., Zou J., Hernando D., Roque R., A. M. W. J. (2021). Investigating the use of Equivalent
501 Elastic Approach to Identify the Potential Location of bending-induced Interface
502 Debonding Under a Moving Load. *Materials and Structures*, 54(18).

503 Pasquini, E., Bocci, M., & Canestrari, F. (2014). Laboratory characterisation of optimised
504 geocomposites for asphalt pavement reinforcement. *Geosynthetics International*, 21(1),
505 24–36. <https://doi.org/10.1680/gein.13.00032>

506 Pasquini, E., Pasetto, M., & Canestrari, F. (2015). Geocomposites against reflective cracking in

507 asphalt pavements: laboratory simulation of a field application. *Road Materials and*
508 *Pavement Design*, 16(4), 815–835. <https://doi.org/10.1080/14680629.2015.1044558>

509 prEN 12697-48. (n.d.). “*Bituminous mixtures – Test methods for hot mix asphalt – Part 48:*
510 *Interlayer Bonding.*”

511 R. Leutner. (1979). Untersuchung des Schichtverbundes beim bituminösen Oberbau. In
512 *Bitumen 3.*

513 Raab, C., Partl, M. N., & El Halim, A. E. H. O. A. (2009). Evaluation of interlayer shear bond
514 devices for asphalt pavements. *Baltic Journal of Road and Bridge Engineering*, 4(4), 186–
515 195. <https://doi.org/10.3846/1822-427X.2009.4.186-195>

516 Ran, W., Zhang, Y., Li, L., Shen, X., Zhu, H., & Zhang, Y. (2019). Characterization of bonding
517 between asphalt concrete layer underwater and salt erosion. *Materials*, 12(19).
518 <https://doi.org/10.3390/ma12193055>

519 Santagata, E., Canestrari, F., & Santagata, F. A. (1993). Laboratory shear testing of tack coat
520 emulsion. *Proceedings of the 1st Congress on Emulsion, Paris, France.*

521 Saride, S., & Kumar, V. V. (2017). Influence of geosynthetic-interlayers on the performance of
522 asphalt overlays on pre-cracked pavements. *Geotextiles and Geomembranes*, 45(3), 184–
523 196. <https://doi.org/10.1016/j.geotextmem.2017.01.010>

524 UNI/TS 11214, (2007). (n.d.). “*Mechanical properties of road and airport pavements. Shear*
525 *performance characterization of interfaces. ASTRA test method.*”

526 Uzan, J., Livneh, M., & Eshed, Y. (1978). Investigation of adhesion properties between
527 asphaltic-concrete layers. *Asphalt Paving Technol*, 495–521.

528 Zamora-Barraza, D., Calzada-Peréz, M., Castro-Fresno, D., & Vega-Zamanillo, A. (2010). New
529 procedure for measuring adherence between a geosynthetic material and a bituminous
530 mixture. *Geotextiles and Geomembranes*, 28(5), 483–489.

531 <https://doi.org/10.1016/j.geotexmem.2009.12.010>

532

533 *Tables*

534 Table 1. Characteristics of Polymer Modified Binder

Binder characteristics	Standard	Unit	Reference values	Measured values
SBS polymer content by weight	-	[%]	3.8	-
Penetration @25°C	EN 1426	[dmm]	50-70	54
Ring and ball softening point	EN 1427	[°C]	≥65	71
Elastic recovery @25°C, 25 cm/min	EN 13398	[%]	≥50	89
Dynamic viscosity @135°C	ASTM D4402	[Pa·s]		1.24
Mass loss after RTFOT	EN 12607-1	[%]	≤0.5	0.1
Penetration @25°C after RTFOT	EN 1426	[%]	≥50	50
Ring and ball softening point after RTFOT	EN 1427	[°C]	≥65	77

535

536

537

538

539

540

541

542

543

544

545

546

547

548

549

550

551

552

553

554 Table 2. Characteristics of the bituminous emulsion for tack coat (EN 13808)

Requirements	Characteristics	Unit	Performance		
			min	max	class
Binder contents	Azeotropic distillation	[%]	53	57	5
Viscosity	Efflux time at 40°C, 2mm	[s]	15	70	3
Breaking Index	Natural filler method		70	155	3
Characteristics of the binder extracted by evaporation					
Consistency at intermediate service temperatures	Penetration at 25°C	dmm		220	5
Consistency at high service temperatures	Softening point	°C	35		8

555

556

557

558

559

560

561

562

563

564

565

566

567

568

569

570

571

572

573

574

575 Table 3. Characteristics of the geocomposites

Property	Geocomposites			
	A	B	C	D
Thickness [mm]	2.5	2.5	1.8/2.5	2.5
Mesh size [mm]	12.5	Non directional	12.5	12.5
Tensile strength L/T [kN/m]	40/40	35/35	40/44	40/40
Elongation at breaking L/T [%]	4/4	30/30	3/3,5	4/4
Geomembrane compound	SBS polymer modified bitumen	SBS polymer modified bitumen	SBS polymer modified bitumen	SBS polymer modified bitumen

576

577

578

579

580

581

582

583

584

585

586

587

588

589

590

591

592

593

594

595 Table 4. Number of specimens tested for Leutner and ASTRA investigation

Specimen type	Lower layer surface condition	Interface configuration				
		N	A	B	C	D
Field	T1	1	2	2	3	3
	T4	3	3	3	3	3
	T6	3	3	3	3	3
Laboratory	T4_lab	2	2	2	2	2

596

597

598

599

600

601

602

603

604

605

606

607

608

609

610

611

612

613

614

615

616

617

618 Table 5. Test results and data analysis for the calculation of α_1 , α_2 and α_3

Section	Interface configuration	$ISS_{Leut50.8}$ (MPa)	$ISS_{Leut2,5}$ (MPa)	$(ISS_{ASTRA})_{meas}$ (MPa)	$(ISS_{ASTRA})_{calc}$ (MPa)
T4	A	0.492	0.171	0.326	0.324
	B	0.516	0.180	0.384	0.333
	C	0.706	0.246	0.372	0.402
	D	0.662	0.231	0.358	0.386
T4_lab	A	0.783	0.273	0.431	0.430
	B	0.997	0.347	0.585	0.507
	C	0.940	0.327	0.423	0.487
	D	1.015	0.354	0.522	0.514

619

620

621

622

623

624

625

626

627

628

629

630

631

632

633

634

635

636

637

638

639 Table 6. ISS specification limits for interfaces reinforced with geocomposites

Phase	Leutner	ASTRA
	@20°C; 50.8 mm/min; 0.0 MPa	@20°C; 2.5 mm/min; 0.2 MPa
Laboratory qualification	≥ 0.75 MPa	≥ 0.42 MPa
In the field	≥ 0.50 MPa	≥ 0.33 MPa

640

641

642

643

644

645

646

647

648

649

650

651

652

653

654

655

656

657

658

659

660

661

662



(a)



(b)

664

665

666 Figure 1. Field trial: (a) milled surface; (b) geocomposite application

667

668

669

670

671

672

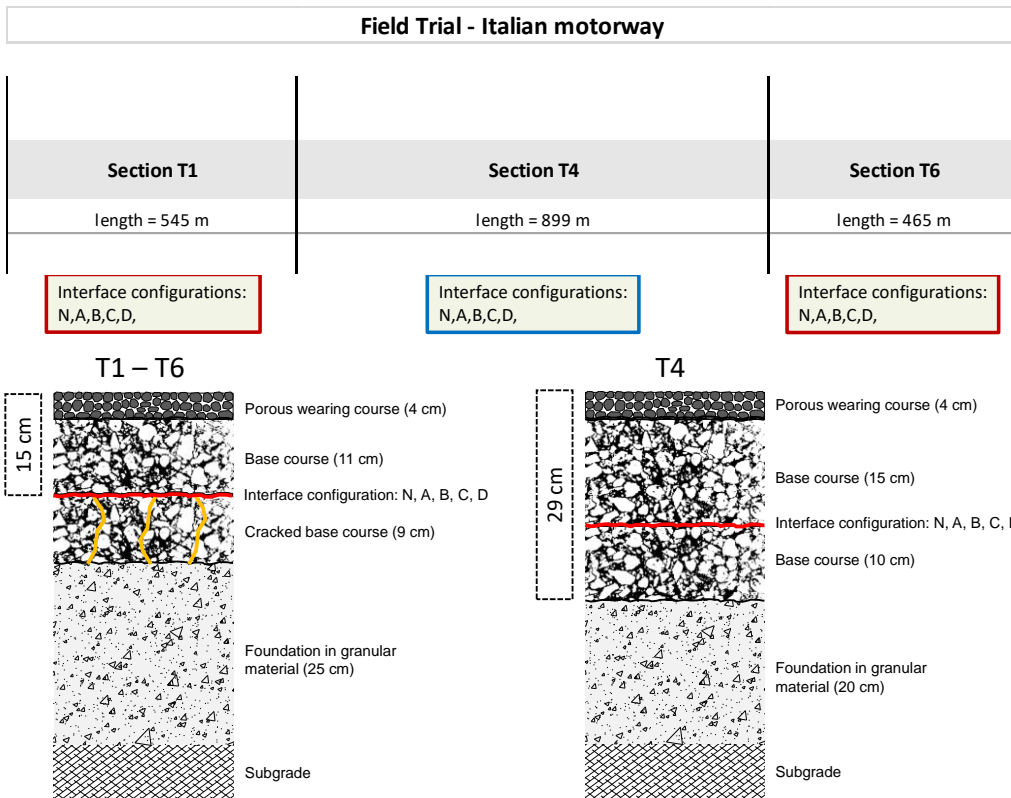
673

674

675

676

677



678

679 Figure 2. Field trial characteristics, stratigraphy and interface configuration

680

681

682

683

684

685

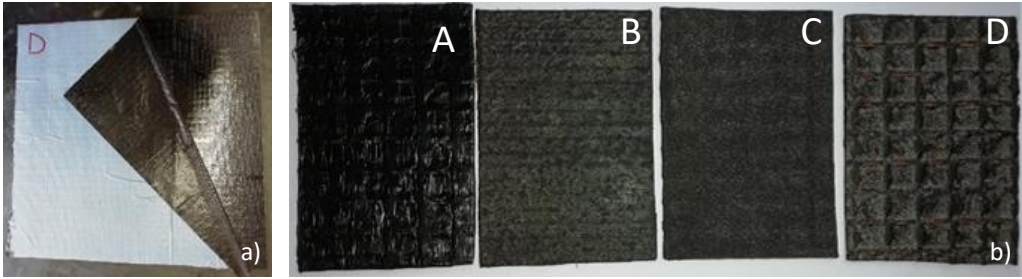
686

687

688

689

690



691

692 Figure 3. Geocomposites: (a) Lower surface; (b) Upper surfaces

693

694

695

696

697

698

699

700

701

702

703

704

705

706

707

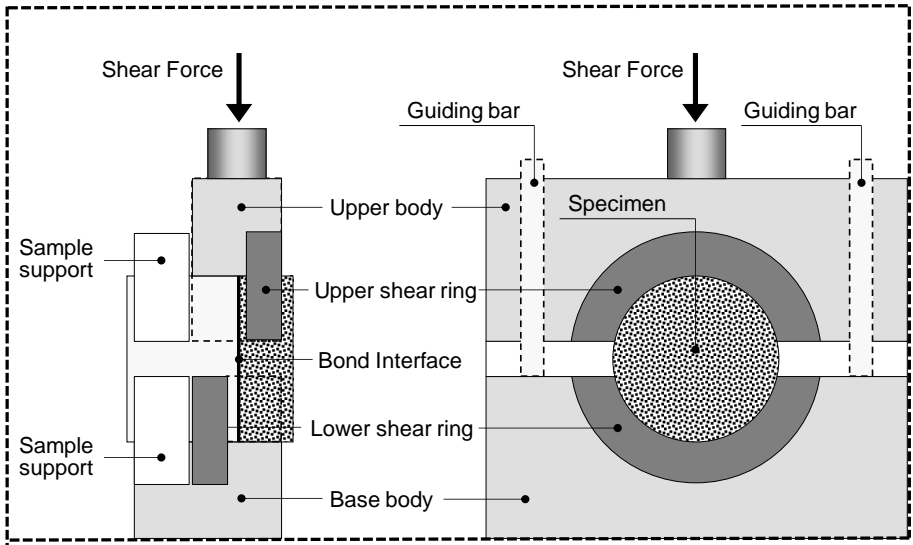
708

709

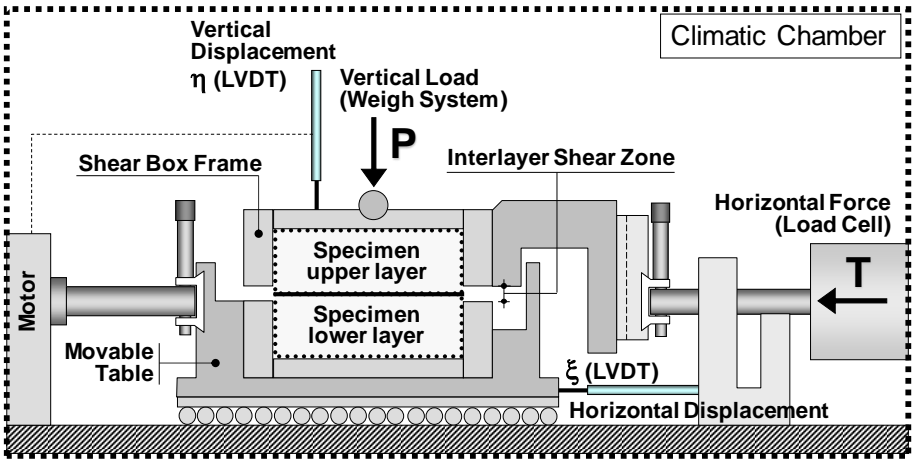
710

711

712



713



714

715 Figure 4. Working scheme: a) Leutner device; b) ASTRA device

716

717

718

719

720

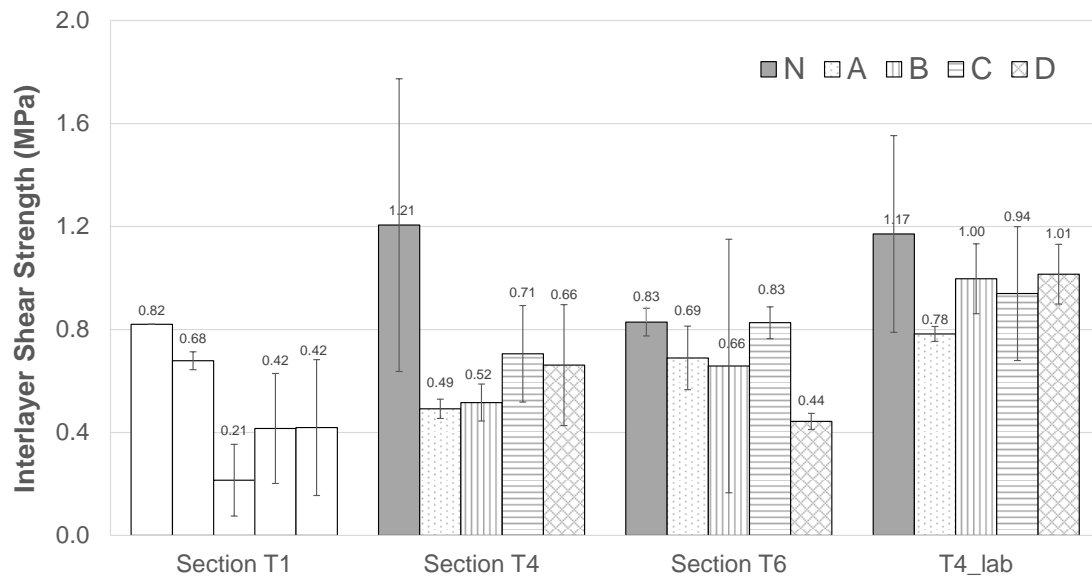
721

722

723

724

725



726

727 Figure 5. Average values of ISS for Leutner test

728

729

730

731

732

733

734

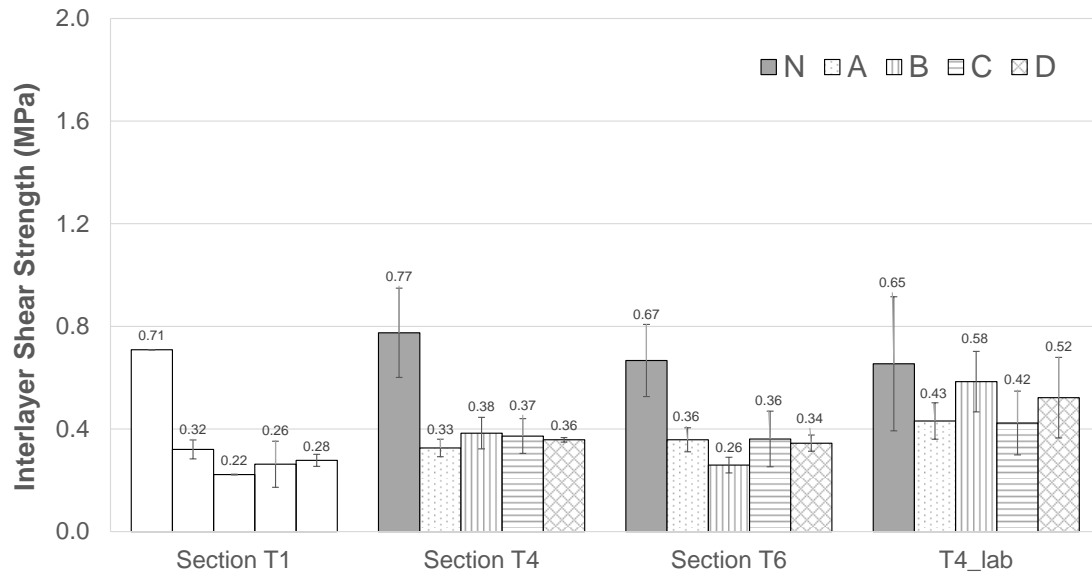
735

736

737

738

739



740

741 Figure 6. Average values of ISS for ASTRA tests

742

743

744

745

746

747

748

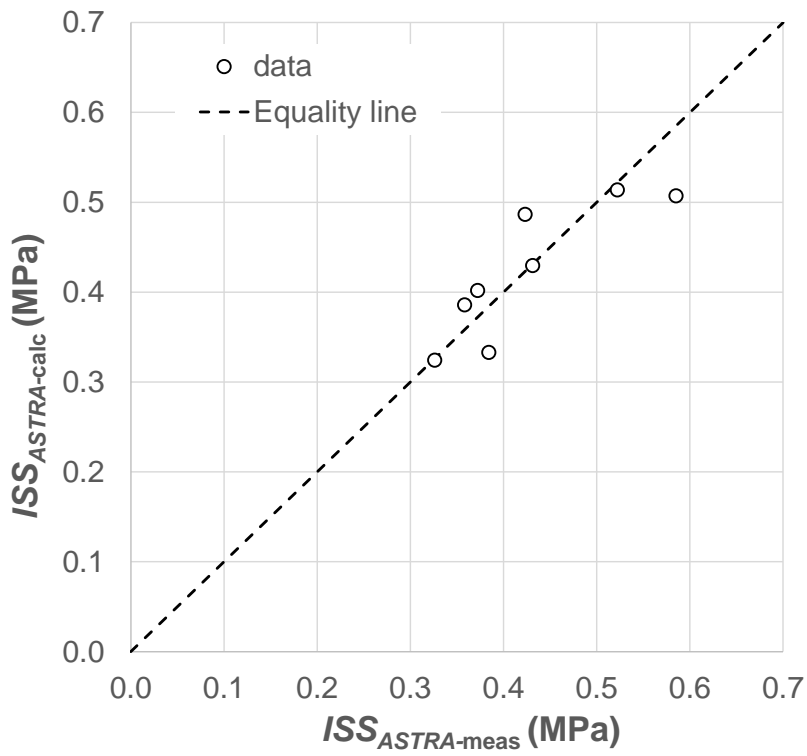
749

750

751

752

753



754

755 Figure 7. Comparison of measured and calculated ISS values for ASTRA tests

756

757

758

759

760

761

762

763

764

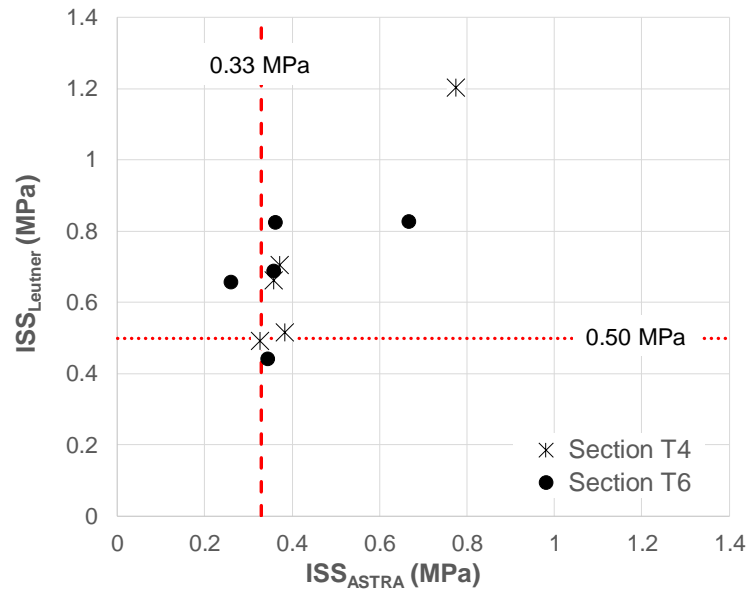
765

766

767

768

769



770

771 Figure 8. ISS for sections T4 and T6 and specification limits for Leutner and ASTRA tests

772

773

774

775

776

777

778

779

780

781

782

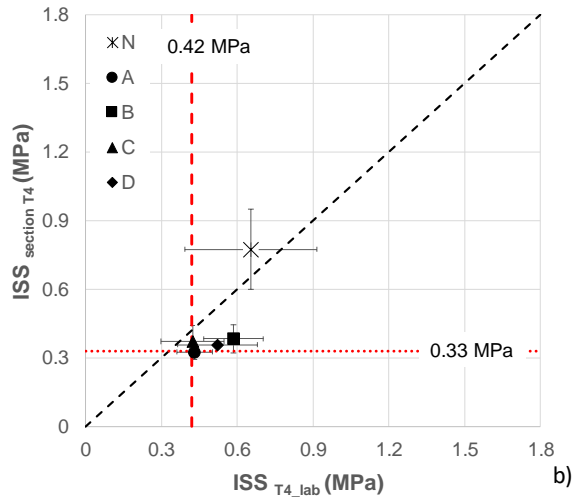
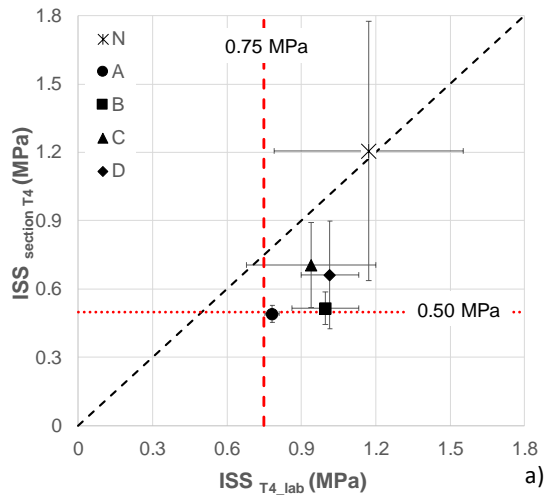
783

784

785

786

787



788

789 Figure 9. Comparison between laboratory and field specimens for the new lower layer surface

790 condition: (a) Leutner; (b) ASTRA